Independent Poor Prognostic Factors for True Progression after Radiation Therapy and Concomitant Temozolomide in Patients with Glioblastoma: Subependymal Enhancement and Low ADC Value

R.-E. Yoo, S.H. Choi, T.M. Kim, S.-H. Lee, C.-K. Park, S.-H. Park, I.H. Kim, T.J. Yun, J.-H. Kim, and C.H. Sohn

ABSTRACT

BACKGROUND AND PURPOSE: Subependymal enhancement and DWI have been reported to be useful MR imaging markers for identifying true progression. Our aim was to determine whether the subependymal enhancement pattern and ADC can differentiate true progression from pseudoprogression in patients with glioblastoma multiforme treated with concurrent chemoradiotherapy by using temozolomide.

MATERIALS AND METHODS: Forty-two patients with glioblastoma multiforme with newly developed or enlarged enhancing lesions on the first follow-up MR images obtained within 2 months of concurrent chemoradiotherapy completion were included. Subependymal enhancement was analyzed for the presence, location, and pattern (local or distant relative to enhancing lesions). The mean ADC value and the fifth percentile of the cumulative ADC histogram were determined. A multiple logistic regression analysis was performed to identify independent factors associated with true progression.

RESULTS: Distant subependymal enhancement (ie, extending >1 cm or isolated from the enhancing lesion) was significantly more common in true progression ($n = 24$) than in pseudoprogression ($n = 18$) ($P = .042$). The fifth percentile of the cumulative ADC histogram was significantly lower in true progression than in pseudoprogression ($P = .014$). Both the distant subependymal enhancement and the fifth percentile of the cumulative ADC histogram were independent factors associated with true progression ($P = .041$ and $P = .033$, respectively). Sensitivity and specificity for the diagnosis of true progression were 83% and 67%, respectively, by using both factors.

CONCLUSIONS: Both the distant subependymal enhancement and the fifth percentile of the cumulative ADC histogram were significant independent factors predictive of true progression.

ABBREVIATIONS: CCRT = concurrent chemoradiotherapy; GBM = glioblastoma multiforme; TMZ = temozolomide; RANO = Response Assessment in Neuro-Oncology

Glioblastoma multiforme (GBM) is the most common form of malignant primary brain tumor in adults,[1] which is notorious for its intrinsic aggressiveness and a dismal prognosis.[2,3] The current standard treatment for GBM is maximal safe tumor resection followed by radiation therapy with concurrent temozolomide (TMZ) and adjuvant TMZ.[4]

Recently, the criteria for assessing therapeutic responses in high-grade gliomas have been updated by the Response Assessment in Neuro-Oncology (RANO) Working Group to address the limitations of the previous guideline.[5] For instance, contrast enhancement, which has been regarded as a surrogate marker for tumor progression, has been reassessed as a nonspecific finding merely reflecting the passage of contrast material across a disrupted blood-tumor barrier.[6-11] In particular, radiologists and clinicians have increasingly recognized the occurrence of progressive MR imaging lesions immediately after completion of concurrent chemoradiotherapy (CCRT) with TMZ, which spontaneously improved without further treatment other than the adjuvant TMZ.[12-14] The treatment-related reaction is termed pseudoprogression and has received attention as a potential pitfall in the response evaluation. At present, owing to the lack of established findings in conventional contrast-enhanced MR imaging for the differential diagnosis of true

Received December 20, 2014; accepted after revision March 2, 2015.

From the Departments of Radiology (R.-E.Y., S.H.C., T.J.Y., J.-H.K, C.H.S) and Pathology (S.-H.P.); Departments of Internal Medicine (S.-H.L., T.M.K.) and Radiation Oncology (C.H.S., I.H.K.), Cancer Research Institute; and Department of Neurosurgery (C.-K.P.), Biomedical Research Institute; Seoul National University College of Medicine, Seoul, Korea; and Center for Nanoparticle Research (R.-E.Y., S.H.C.), Institute for Basic Science and School of Chemical and Biological Engineering (R.-E.Y., S.H.C.), Seoul National University, Seoul, Korea.

This study was supported by a grant from the Korea Healthcare Technology R&D Projects, Ministry for Health, Welfare and Family Affairs (HI13C0015), and the Research Center Program of Institute for Basic Science in Korea.

Please address correspondence to Seung Hong Choi, MD, PhD, Department of Radiology, Seoul National University College of Medicine, 28, Yongon-dong, Chongno-gu, 110–744, Seoul, Korea; Center for Nanoparticle Research, Institute for Basic Science and School of Chemical and Biological Engineering, Seoul National University, 1 Gwanak-ro, Gwanak-gu, 151–742, Seoul, Korea; e-mail: verocay@snuh.org

Indicates open access to non-subscribers at www.ajnr.org

Indicates article with supplemental on-line photo.

http://dx.doi.org/10.3174/ajnr.A4401

progression from pseudoprogression,[9,10] RANO stresses that the diagnosis of true progression can be made within the first 12 weeks after completion of radiation therapy only if most of the new enhancement is located outside the radiation field or if there is pathologic confirmation of progressive disease.[5]

During the past few decades, there has been extensive effort to identify imaging biomarkers for tumor progression. Among the many parameters derived from advanced MR imaging techniques, DWI has been consistently reported to be helpful in differentiating tumor progression from treatment-related changes or necrosis.[15-22] Meanwhile, most previous studies pertaining to the role of conventional MR imaging have not shown promising results.[9,23] Nevertheless, a recent study focusing on the conventional MR imaging findings has proposed subependymal enhancement as a useful MR imaging marker for differentiating true progression from pseudoprogression.[24] To our knowledge, however, no previous studies have conducted in-depth analysis of the subependymal enhancement, and its potential as an independent predictor for true progression remains elusive.

The purpose of the present study was to determine whether the subependymal enhancement pattern and ADC can differentiate true progression from pseudoprogression in patients with GBM treated with radiation therapy and concomitant TMZ.

MATERIALS AND METHODS

This retrospective study was approved by our institutional review board, and informed consent was waived.

Patient Selection

One hundred thirty-two patients with newly diagnosed GBM, who had undergone surgical resection or stereotactic biopsy at our institution between June 2008 and March 2013 were selected from our radiology report data base. The inclusion criteria were patients with the following: 1) histopathologic diagnosis of GBM according to the World Health Organization criteria; 2) CCRT with TMZ and 6 cycles of adjuvant TMZ performed after surgical resection or biopsy; 3) baseline contrast-enhanced MR imaging performed within 24–48 hours after surgery before CCRT with TMZ; 4) the first follow-up 3T MR imaging including DWI (b=1000 s/mm^2) performed within 2 months (mean, 28 days; range, 12–62 days) after the end of CCRT; 5) newly developed or enlarged measurable contrast-enhancing lesions inside the radiation field on the first follow-up MR images; and 6) follow-up contrast-enhanced MR imaging after 6 cycles of adjuvant TMZ to confirm true progression or pseudoprogression. The measurable contrast-enhancing lesions were defined as bidimensional contrast-enhancing lesions with 2 perpendicular diameters of at least 10 mm.[5] We excluded 88 patients for the following reasons: 1) poor quality of the MR images, 2) no newly visible enhancing lesions on the first follow-up MR images, 3) definite disease progression according to the RANO criteria, and 4) the presence of subependymal enhancement on the baseline MR images.[5] Two additional patients were excluded because of follow-up loss in one and a switch to bevacizumab in the other (Fig 1).

Therefore, 42 patients (27 men, 15 women; mean age, 56 years; age range, 28–80 years) were included in this study. After adjuvant TMZ, true progression and pseudoprogression were confirmed in 24 and 18 patients, respectively, by our neuro-oncology team (consisting of radiologists, neurosurgeons, neuro-oncologists, and radiation oncologists) according to the RANO criteria (Fig 1).[5] Clinical characteristics of the patients, including age, sex, Karnofsky performance score (at the time of the first follow-up MR imaging), methylation status of O6-methylguanine DNA methyltransferase promoter of the tumor, surgical method, and radiation dose of the CCRT, were documented.

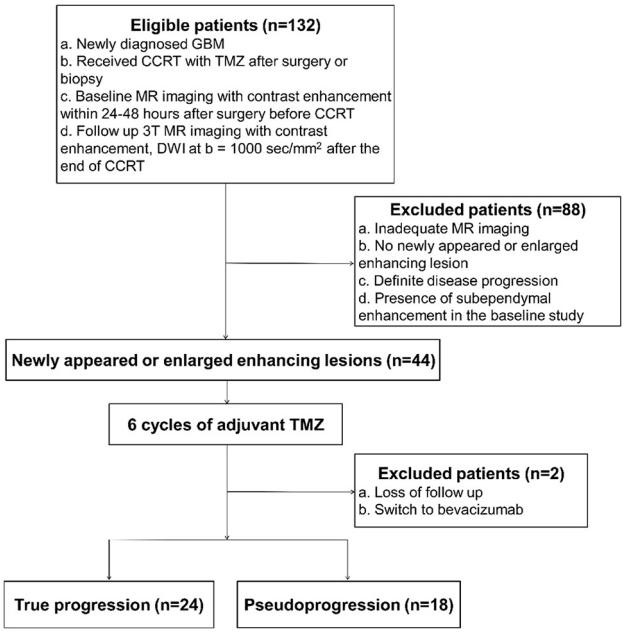

FIG 1. Flow diagram of patient selection, with inclusion and exclusion criteria.

Image Acquisition

For all cases, the first follow-up MR imaging studies after the completion of CCRT with TMZ were performed with 1 of two 3T MR imaging scanners (Signa Excite; GE Healthcare, Milwaukee, Wisconsin [true progression, n = 6; pseudoprogression, n = 3]; Magnetom Verio; Siemens, Erlangen, Germany [true progression, n = 18; pseudoprogression, n = 15]) with an 8-channel head coil.

The imaging protocol included 3D magnetization-prepared rapid acquisition of gradient echo, axial TSE T2WI, axial FLAIR imaging, and DWI. Echo-planar DWI was performed in the axial plane before contrast material injection. Diffusion-weighted images were acquired in 3 orthogonal directions and combined into a trace image. By using these data, we calculated ADC maps at b-values of 0 and 1000 s/mm^2 on a voxel-by-voxel basis with software incorporated into the MR imaging unit. Axial spin-echo T1WI was repeated after intravenous administration of a single dose (0.1 mmol per kilogram of body weight) of gadobutrol (Gadovist; Bayer Schering Pharma, Berlin, Germany). A standard dose of 0.1 mmol/kg body weight of a gadolinium-based contrast agent (Gadovist) was injected intravenously at a rate of 5 mL/s, followed by a 20-mL bolus of saline at a rate of 5 mL/s by using a power injector (Optistar; Mallinckrodt, St Louis, Missouri). A fat-suppression pulse was added to the axial T1WI after administration of the contrast agent. Specific imaging parameters for the sequences are provided in Table 1.

Table 1: MR imaging parameters

Parameters	3D MPRAGE	Axial TSE T2WI	FLAIR	DWI
TR (ms)	1500	4500–5160	9000–9902	6900–10,000
TE (ms)	1.9	91–106	97–163	55–67
TI (ms)	900	NA	2500	NA
Echo-train length	1	16–19	0–11	1
Flip angle (degree)	9	90–130	90–130	90
Section thickness (mm)	1	5	5	3–5
Intersection gap (mm)	0	1	1	0.9–1
FOV (mm)	250 × 250	199–220 × 220	199–220 × 220	240 × 240
Matrix	256 × 256	448–640 × 256–290	320–384 × 192–209	160 × 160
No. of signals acquired	1	0–2	0–1	0–3
No. of sections	192	25	25	50–70

Note:—NA indicates not available.

Qualitative Image Analysis for Subependymal Enhancement

Two neuroradiologists (S.H.C. and J.-H.K. with 7 and 15 years of experience, respectively, in the interpretation of MR imaging studies), who were blinded as to whether the patients had true progression or pseudoprogression, analyzed the first follow-up MR images together and reached a consensus reading for subependymal enhancement in terms of the following: 1) the presence or absence, 2) location, and 3) pattern of enhancement. Regarding the pattern, the subependymal enhancement was categorized into 1 of the following, according to the positional relationship between the subependymal enhancement and an enhancing lesion: 1) type I: enhancement at the ependymal lining abutting the newly developed or enlarged measurable contrast-enhancing lesion; 2) type II: enhancement extending along the ventricular margin with the distance of extension (ie, distance from the margin of the enhancing lesion to the farthest end of the subependymal enhancement) measuring ≤1 cm; 3) type III: enhancement extending along the ventricular margin with the distance of extension measuring >1 cm; and 4) type IV: enhancement at the ependymal lining isolated from the enhancing lesion. Type I and II patterns were classified as local, whereas type III and IV patterns were classified as distant (On-line Fig 1).

Quantitative Image Analysis for ADC Maps

The MR imaging data for ADC maps were digitally transferred from the PACS workstation to a personal computer. ROIs that contained the entire measurable contrast-enhancing lesions, excluding the areas of necrosis or cysts, were manually drawn in each section of the ADC maps by 1 neuroradiologist (R.-E.Y. with 5 years of experience in the interpretation of MR imaging studies) by using ImageJ software (National Institutes of Health, Bethesda, Maryland). The data acquired from each section were summated to derive voxel-by-voxel ADC values for the entire contrast-enhancing lesions by using software developed in house.

Subsequently, the mean ADC values were calculated. For further quantitative analysis, the fifth percentiles (the point at which 5% of the voxel values that form the cumulative ADC histogram are found to the left) were calculated on the basis of the previous finding that the fifth percentile of the cumulative ADC histogram was a significant predictor for the differential diagnosis between true progression and pseudoprogression.[17,21]

Statistical Analysis

All statistical analyses were performed by using the statistical software MedCalc for Windows, Version 11.1.1.0 (MedCalc Software, Mariakerke, Belgium). The data for each parameter were assessed for normality with the Kolmogorov-Smirnov test. In all tests, P values $< .05$ were considered statistically significant.

Clinical characteristics of the patients in the 2 groups were compared by using either the Fisher exact test or the unpaired Student t test. The Fisher exact test was performed to assess whether the incidence of the subependymal enhancement significantly differed between the true progression and pseudoprogression groups. The unpaired Student t test was used to compare the mean ADC values and the fifth percentiles of the cumulative ADC histograms between the 2 groups. Variables showing a univariate association with true progression (at $P < .10$) were included in a multivariable stepwise logistic regression analysis to identify independent predictors of true progression.

Sensitivity and specificity of the imaging parameters for the diagnosis of true progression were calculated. To determine an optimal cutoff value that provided a balance between sensitivity and specificity, a receiver operating characteristic curve was constructed for the ADC values. In addition, a leave-one-out cross-validation method was used to test the effects of outliers.[25]

RESULTS

Clinical Characteristics of the Patients

There was a significant difference in age between the true progression and pseudprogression groups ($P = .002$). Other clinical characteristics did not significantly differ between the 2 groups (Table 2).

Qualitative Image Analysis for Subependymal Enhancement

Subependymal enhancement was significantly more common in the true progression group (19 of 24) than in the pseudoprogression group (8 of 18) ($P = .027$). Anatomic locations of the subependymal enhancement were as follows: unilateral lateral ventricle ($n = 25$), bilateral lateral ventricles ($n = 1$), and fourth ventricle ($n = 1$). With regard to the pattern, the incidence of distant subependymal enhancement was significantly higher in the true progression group than in the pseudoprogression group ($P = .042$), whereas that of local subependymal enhancement did not significantly differ between the 2 groups ($P > .99$) (Table 3 and Fig 2).

Quantitative Image Analysis for ADC Maps

The fifth percentile of the cumulative ADC histogram was significantly lower in the true progression group than in the pseudoprogression group (895×10^{-6} mm^2/s versus 998×10^{-6} mm^2/s, $P = .014$). In contrast, the mean ADC value was not significantly different between the 2 groups (1247×10^{-6} mm^2/s versus 1310×10^{-6} mm^2/s, $P = .298$) (Table 3).

Table 2. Clinical characteristics of the patients

Characteristic	True Progression (n = 24)	Pseudoprogression (n = 18)	P Value
Age (yr)	60.50 ± 11.58	48.22 ± 12.54	.002
Sex			.347
Male	17	10	
Female	7	8	
Karnofsky performance score			.371
<70	4	1	
≥70	20	17	
Surgery			.623
Biopsy	3	1	
Resection	21	17	
Radiation dose (Gy)	55.52 ± 8.17	57.83 ± 7.52	.376
Methylated MGMT promoter[a]			1.000
Negative	6	5	
Positive	15	13	

Note:—MGMT indicates O6-methylguanine DNA methyltransferase.

[a] The promoter methylation status of MGMT, which was investigated by using the methylation-specific polymerase chain reaction technique, was documented whenever available.

Table 3: Qualitative and quantitative image analyses[a]

	True Progression (n = 24)	Pseudoprogression (n = 18)	P Value
Subependymal enhancement	19 (79)	8 (44)	.027
Local	9 (38)	6 (33)	>.99
Type I	8 (33)	4 (22)	
Type II	1 (4)	2 (11)	
Distant	10 (42)	2 (11)	.042
Type III	5 (21)	0 (0)	
Type IV	5 (21)	2 (11)	
ADC ($\times 10^{-6}$ mm^2/s)			
Mean	1247 ± 197	1310 ± 182	.298
Fifth percentile	895 ± 136	998 ± 120	.014

[a] Numbers in parentheses are percentages.

Multiple Logistic Regression Analysis for Independent Variables

The multiple logistic regression analysis revealed that age, the distant subependymal enhancement, and the fifth percentile of the cumulative ADC histogram were independent predictors of true progression (OR, 1.08; 95% CI, 1.01–1.17; $P = .026$ for the age; OR, 8.30; 95% CI, 1.09–63.16; $P = .041$ for the distant subependymal enhancement; and OR, 0.99; 95% CI, 0.98–1.00; $P = .033$ for the fifth percentile of the cumulative ADC histogram) (Fig 3).

Sensitivity and Specificity for the Diagnosis of True Progression with Imaging Parameters

Sensitivity and specificity for the diagnosis of true progression were 42% (95% CI, 24–61) and 89% (95% CI, 67–97), respectively, when considering only distant subependymal enhancement. Sensitivity and specificity were 67% (95% CI, 45–84) and 78% (95% CI, 52–94), respectively, when using only the optimal cutoff ADC value (fifth percentile of the cumulative ADC histogram) of 915×10^{-6} mm^2/s.

The predictive equation was calculated with the 2 logistic regression parameters as

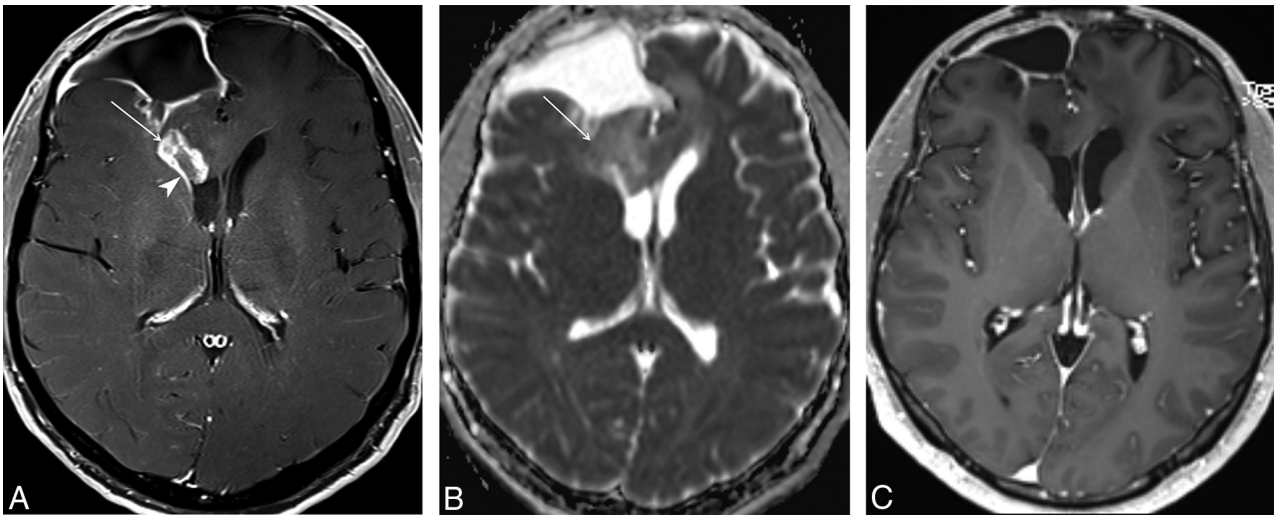

FIG 2. Pseudoprogression in a 40-year-old man with glioblastoma who had undergone surgical resection. *A*, Axial contrast-enhanced T1-weighted MR image obtained within 1 month after the end of concurrent chemotherapy and radiation therapy shows a newly developed enhancing lesion (*arrow*) in the right frontal periventricular white matter. The ventricular margin adjacent to the enhancing lesion (*arrow*) also shows linear enhancement (*arrowhead*), with the distance of extension measuring ≤1 cm. *B*, On the ADC map, a decrease in ADC value is not apparent at the lesion (*arrow*) (mean, 1264×10^{-6} mm^2/s; fifth percentile, 1059×10^{-6} mm^2/s). *C*, Follow-up MR image after a 6-month continuation of temozolomide reveals resolution of the enhancing lesion.

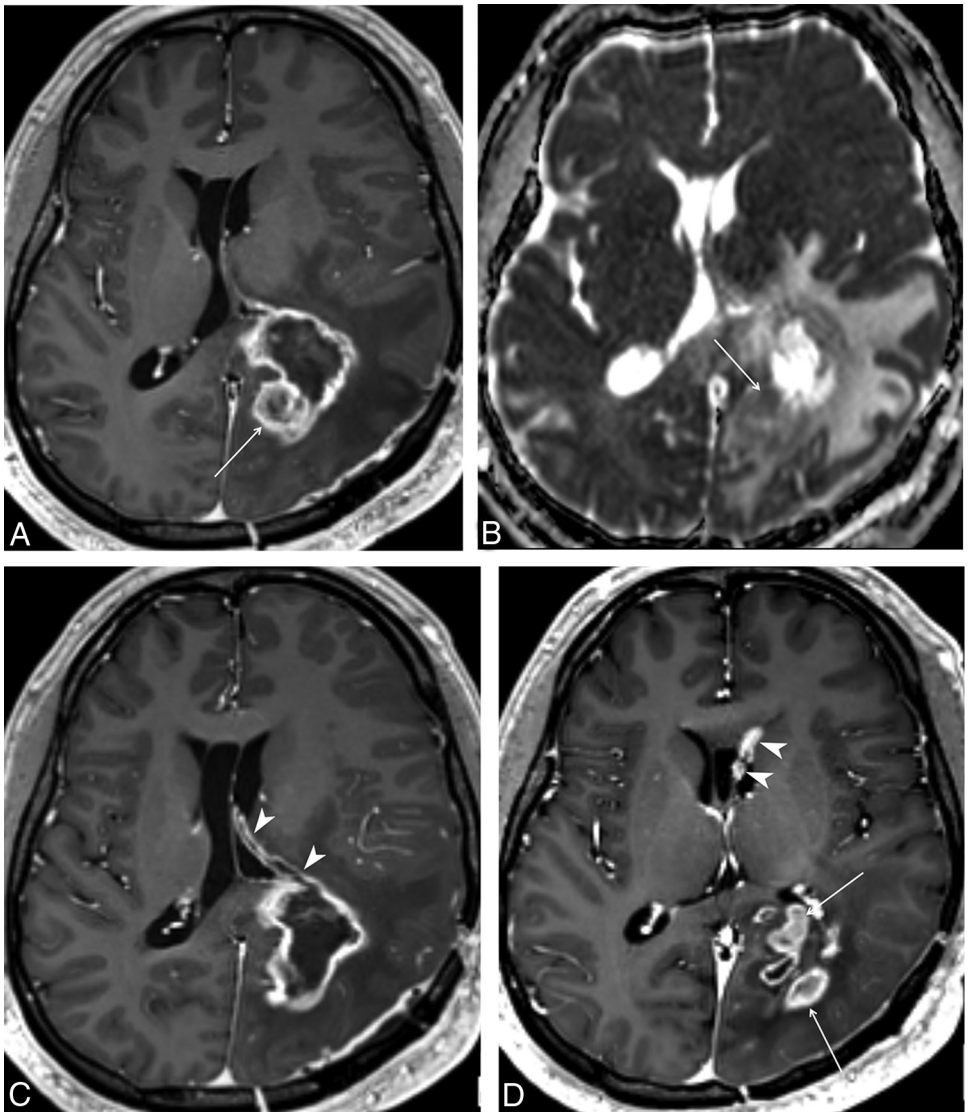

FIG 3. True progression in a 36-year-old man with glioblastoma who had undergone surgical resection. *A*, On the axial contrast-enhanced T1-weighted MR image obtained within 1 month after the end of concurrent chemotherapy and radiation therapy, a newly developed enhancing lesion (*arrow*) is noted in the left occipital lobe. *B*, On the ADC map, the ADC value is decreased in some portion of the lesion (*arrow*) (mean, 1292×10^{-6} mm^2/s; fifth percentile, 991×10^{-6} mm^2/s). *C*, Axial contrast-enhanced T1-weighted MR image at a higher level reveals linear enhancement (*arrowheads*) along the ventricular margin, with the distance of extension measuring >1 cm. *D*, Follow-up MR image after a 6-month continuation of temozolomide demonstrates aggravation of both the left occipital lobe lesion (*arrows*) and subependymal enhancement (*arrowheads*) in the left lateral ventricle.

follows: $P = e^X / (1 + e^X)$, where $\chi = -0.0085 \times$ (fifth percentile of the cumulative ADC histogram) $+ 2.2808 \times$ (distant subependymal enhancement) $+ 7.8108$. The cutoff point for the diagnosis of true progression was defined as a probability value $\geq .50$. The sensitivity, specificity, and accuracy of the equation were 83% (20 of 24), 67% (12 of 18), and 76% (32 of 42), respectively. Leave-one-out cross-validation revealed a sensitivity of 79% (19 of 24), a specificity of 61% (11 of 18), and an accuracy of 71% (30 of 42).

DISCUSSION

Our results demonstrated the value of using the subependymal enhancement pattern and DWI to differentiate true progression from pseudoprogression in patients with GBM treated with CCRT by using TMZ.

Along with the increasing recognition of pseudoprogression, there has been a growing interest in ADC values as surrogate markers for differentiating true progression from pseudoprogression.[15-22] Previous studies found that the fifth percentile of the cumulative ADC histogram based on the entire newly developed or enlarged enhancing lesion could be used to accurately differentiate them.[17,21] Specifically, Chu et al[17] reported a sensitivity of 73% and a specificity of 73% for diagnosing true progression, by using a cutoff ADC value of 929×10^{-6} mm^2/s. Our results showed that the fifth percentile value was significantly lower in the true progression group than in the pseudoprogression group ($P = .014$), while the mean value was not significantly different between the 2 groups—findings in keeping with those of the previous study. With a cutoff ADC value of 915×10^{-6} mm^2/s, sensitivity and specificity for the diagnosis of true progression were 67% and 78%, respectively.

With the advent of various advanced MR imaging techniques, conventional MR imaging has been thought to have a

limited role in the differential diagnosis of true progression from pseudoprogression.[9,23] Nonetheless, some authors have suggested that certain conventional MR imaging findings may be helpful for differentiating them. Mullins et al[23] reported that though individual enhancement patterns such as subependymal enhancement did not show a statistically significant difference between tumor recurrence and radiation necrosis, their combinations—specifically, corpus callosum involvement in conjunction with multiple enhancing lesions with or without crossing of the midline and subependymal spread—favored predominant glioma progression.

More recently, Young et al[24] investigated the potential utility of various conventional MR imaging signs in a larger patient population. The study, unlike that by Mullins et al,[23] included those with worsening (new or increased) enhancing lesions on the initial postradiotherapy MR imaging (usually 2–4 weeks after completion of radiotherapy) and found that the incidence of subependymal enhancement was significantly higher in the early progression group than in the pseudoprogression group ($P = .001$). In agreement with the previous findings, the present study found subependymal enhancement significantly more common in the true progression group than in the pseudoprogression group ($P = .027$). Subependymal spread of tumor, albeit less common than local progression, is a known pattern of glioma failure, with reported rates ranging from 0% to 24%.[26,27] According to previous studies, even though the recurrence pattern of GBM after CCRT was predominantly central at first, distant recurrences, including subependymal spread, often developed during the patient's clinical course.[28,29] It has been speculated that the infiltration of the ventricular margin may occur either by direct spread of tumor cells in the subependymal space or by deposits transferred by the CSF.[30]

Unlike the study by Young et al,[24] we further analyzed the subependymal enhancement in terms of its pattern and found that only the distant subependymal enhancement was significantly more common in the true progression group than in the pseudoprogression group ($P = .042$). The occurrence of local subependymal enhancement in pseudoprogression may be attributed to treatment-related necrosis. The periventricular region is known to be supplied by long medullary arteries with no collateral vessels. It has been suggested that the relatively poor vascularity may predispose the periventricular region to radiation-induced vasculopathy.[9] Furthermore, the periventricular region close to a newly developed contrast-enhancing lesion may be more prone to radiation necrosis because the radiation dose delivered to a specific region during intensity-modulated radiation therapy decreases with increasing distance from the center of the enhancing lesion.[31,32] On the basis of the findings, we infer that the local subependymal enhancement is more likely to reflect radiation necrosis, compared with the distant subependymal enhancement.

Sensitivity and specificity for the diagnosis of true progression were 42% and 89%, respectively, by using only the distant subependymal enhancement. Although the specificity is relatively high, the clinical utility of the imaging findings may be limited due to its low sensitivity. However, our results suggest that the distant subependymal enhancement, when present, can be an early clue to the diagnosis of true progression.

Moreover, the multiple logistic regression analysis revealed that the distant subependymal enhancement and the fifth percentile of the cumulative ADC histogram were independently predictive of true progression (OR, 8.30; $P = .041$; OR, 0.99; $P = .033$, respectively). Given that the enhancing portion presumably represents a wide spectrum of histologic features comprising normal brain tissue, radiation necrosis, and highly cellular recurrent tumor, we infer that the enhancing lesion with the high fifth percentile value may also contain small foci of viable tumor with low ADC values. Hence, we speculate that the incidence of distant subependymal enhancement is likely to be influenced by multiple factors, including the anatomic location of the viable tumor portion within the enhancing lesion (ie, whether it is close to the ventricular margin), not just by the fifth percentile value itself. The sensitivity and specificity for the diagnosis of true progression were 83% and 67%, respectively, by using both independent factors.

Apart from the intrinsic limits of any retrospective study, several other limitations should be mentioned. First, MR imaging was performed on 2 different 3T MR imaging units. However, MR images were optimized to maintain the image quality and to minimize differences between the 2 units. Second, although any discernible necrotic or cystic area was excluded from ROI measurements, it was difficult to eliminate the possibility of including small necrotic or cystic areas. Nonetheless, the contamination was presumed to have had a negligible effect on our results because we used the fifth percentile of the cumulative ADC histogram as the main parameter, rather than the mean value. Third, the present study included a relatively small patient population, in which we could not find any statistically significant difference in the methylation status of O6-methylguanine DNA methyltransferase promoter between the true progression and pseudoprogression groups. On the other hand, the age of the patients was unexpectedly found to be an independent predictor of true progression. A further study with a larger population is warranted to strengthen the statistical power. Fourth, given the possibilities of the occurrence of pseudoprogression later than 3 months after the end of CCRT and coexistence of the 2 entities, some ambiguity may be inevitably present in the final diagnosis of true progression or pseudoprogression because the diagnosis was made on the basis of the follow-up MR images rather than pathologic confirmation. Fifth, there may have been false-negative results for subtle subependymal enhancement because high-resolution volumetric T1-weighted images were not available in some patients from the early study period.

CONCLUSIONS

Both the distant subependymal enhancement (ie, extending >1 cm or isolated from the enhancing lesion) and the fifth percentile of the cumulative ADC histogram of enhancing lesions were significant independent predictors for true progression in patients with GBM. Compared with the histogram analysis of ADC values, the visual assessment of subependymal enhancement is relatively straightforward and less time-consuming. In clinical practice, despite the inherent difficulty of differentiating true progression from pseudoprogression, the diagnostic accuracy may be im-

proved by taking into account both the subependymal enhancement pattern and ADC values.

Disclosures: Seung Hong Choi—*RELATED*: *Grant*: Korea Healthcare Technology R&D Projects, Ministry for Health, Welfare and Family Affairs (HI13C0015), and the Research Center Program of Institute for Basic Science in Korea.* *Money paid to the institution.

REFERENCES

1. Wen PY, Kesari S. **Malignant gliomas in adults.** *N Engl J Med* 2008;359:492–507
2. Brandes AA, Tosoni A, Spagnolli F, et al. **Disease progression or pseudoprogression after concomitant radiochemotherapy treatment: pitfalls in neurooncology.** *Neuro Oncol* 2008;10:361–67
3. Jeon HJ, Kong DS, Park KB, et al. **Clinical outcome of concomitant chemoradiotherapy followed by adjuvant temozolomide therapy for glioblastaomas: single-center experience.** *Clin Neurol Neurosurg* 2009;111:679–82
4. Stupp R, Mason WP, van den Bent MJ, et al; European Organisation for Research and Treatment of Cancer Brain Tumor and Radiotherapy Groups, National Cancer Institute of Canada Clinical Trials Group. **Radiotherapy plus concomitant and adjuvant temozolomide for glioblastoma.** *N Engl J Med* 2005;352:987–96
5. Wen PY, Macdonald DR, Reardon DA, et al. **Updated response assessment criteria for high-grade gliomas: Response Assessment in Neuro-Oncology Working Group.** *J Clin Oncol* 2010;28:1963–72
6. Cairncross JG, Macdonald DR, Pexman JH, et al. **Steroid-induced CT changes in patients with recurrent malignant glioma.** *Neurology* 1988;38:724–26
7. Finn MA, Blumenthal DT, Salzman KL, et al. **Transient postictal MRI changes in patients with brain tumors may mimic disease progression.** *Surg Neurol* 2007;67:246–50; discussion 250
8. Henegar MM, Moran CJ, Silbergeld DL. **Early postoperative magnetic resonance imaging following nonneoplastic cortical resection.** *J Neurosurg* 1996;84:174–79
9. Kumar AJ, Leeds NE, Fuller GN, et al. **Malignant gliomas: MR imaging spectrum of radiation therapy- and chemotherapy-induced necrosis of the brain after treatment.** *Radiology* 2000;217:377–84
10. Ulmer S, Braga TA, Barker FG 2nd, et al. **Clinical and radiographic features of peritumoral infarction following resection of glioblastoma.** *Neurology* 2006;67:1668–70
11. Watling CJ, Lee DH, Macdonald DR, et al. **Corticosteroid-induced magnetic resonance imaging changes in patients with recurrent malignant glioma.** *J Clin Oncol* 1994;12:1886–89
12. Brandsma D, Stalpers L, Taal W, et al. **Clinical features, mechanisms, and management of pseudoprogression in malignant gliomas.** *Lancet Oncol* 2008;9:453–61
13. Chaskis C, Neyns B, Michotte A, et al. **Pseudoprogression after radiotherapy with concurrent temozolomide for high-grade glioma: clinical observations and working recommendations.** *Surg Neurol* 2009;72:423–28
14. Taal W, Brandsma D, de Bruin HG, et al. **Incidence of early pseudoprogression in a cohort of malignant glioma patients treated with chemoirradiation with temozolomide.** *Cancer* 2008;113:405–10
15. Abdel Razek AA, Kandeel AY, Soliman N, et al. **Role of diffusion-weighted echo-planar MR imaging in differentiation of residual or recurrent head and neck tumors and posttreatment changes.** *AJNR Am J Neuroradiol* 2007;28:1146–52
16. Asao C, Korogi Y, Kitajima M, et al. **Diffusion-weighted imaging of radiation-induced brain injury for differentiation from tumor recurrence.** *AJNR Am J Neuroradiol* 2005;26:1455–60
17. Chu HH, Choi SH, Ryoo I, et al. **Differentiation of true progression from pseudoprogression in glioblastoma treated with radiation therapy and concomitant temozolomide: comparison study of standard and high-b-value diffusion-weighted imaging.** *Radiology* 2013;269:831–40
18. Hein PA, Eskey CJ, Dunn JF, et al. **Diffusion-weighted imaging in the follow-up of treated high-grade gliomas: tumor recurrence versus radiation injury.** *AJNR Am J Neuroradiol* 2004;25:201–09
19. Lee WJ, Choi SH, Park CK, et al. **Diffusion-weighted MR imaging for the differentiation of true progression from pseudoprogression following concomitant radiotherapy with temozolomide in patients with newly diagnosed high-grade glioma.** *Acad Radiol* 2012;19:1353–61
20. Matsusue E, Fink JR, Rockhill JK, et al. **Distinction between glioma progression and post-radiation change by combined physiologic MR imaging.** *Neuroradiology* 2010;52:297–306
21. Song YS, Choi SH, Park CK, et al. **True progression versus pseudoprogression in the treatment of glioblastomas: a comparison study of normalized cerebral blood volume and apparent diffusion coefficient by histogram analysis.** *Korean J Radiol* 2013;14:662–72
22. Cha J, Kim ST, Kim HJ, et al. **Differentiation of tumor progression from pseudoprogression in patients with posttreatment glioblastoma using multiparametric histogram analysis.** *AJNR Am J Neuroradiol* 2014;35:1309–17
23. Mullins ME, Barest GD, Schaefer PW, et al. **Radiation necrosis versus glioma recurrence: conventional MR imaging clues to diagnosis.** *AJNR Am J Neuroradiol* 2005;26:1967–72
24. Young RJ, Gupta A, Shah AD, et al. **Potential utility of conventional MRI signs in diagnosing pseudoprogression in glioblastoma.** *Neurology* 2011;76:1918–24
25. Man MZ, Dyson G, Johnson K, et al. **Evaluating methods for classifying expression data.** *J Biopharm Stat* 2004;14:1065–84
26. Kyritsis AP, Levin VA, Yung WK, et al. **Imaging patterns of multifocal gliomas.** *Eur J Radiol* 1993;16:163–70
27. Sneed PK, Gutin PH, Larson DA, et al. **Patterns of recurrence of glioblastoma multiforme after external irradiation followed by implant boost.** *Int J Radiat Oncol Biol Phys* 1994;29:719–27
28. Milano MT, Okunieff P, Donatello RS, et al. **Patterns and timing of recurrence after temozolomide-based chemoradiation for glioblastoma.** *Int J Radiat Oncol Biol Phys* 2010;78:1147–55
29. Ogura K, Mizowaki T, Arakawa Y, et al. **Initial and cumulative recurrence patterns of glioblastoma after temozolomide-based chemoradiotherapy and salvage treatment: a retrospective cohort study in a single institution.** *Radiat Oncol* 2013;8:97
30. McGeachie RE, Gold LH, Latchaw RE. **Periventricular spread of tumor demonstrated by computed tomography.** *Radiology* 1977;125:407–10
31. Ammirati M, Chotai S, Newton H, et al. **Hypofractionated intensity modulated radiotherapy with temozolomide in newly diagnosed glioblastoma multiforme.** *J Clin Neurosci* 2014;21:633–37
32. Burnet NG, Jena R, Burton KE, et al. **Clinical and practical considerations for the use of intensity-modulated radiotherapy and image guidance in neuro-oncology.** *Clin Oncol (R Coll Radiol)* 2014;26:395–406